Structural fluctuations and quantum transport through DNA molecular wires: a combined molecular dynamics and model Hamiltonian approach

R. Gutiérrez and G. Cuniberti

Institute for Materials Science and Max Bergmann Center of Biomaterials,
Dresden University of Technology, 01062, Dresden, Germany

R. Caetano

Instituto de Fisica, Universidade Federal de Alagoas, Maceio, AL 57072-970, Brazil

P. B. Woiczikowski and M. Elstner

Institute for Physical Chemistry, University Karlsruhe, 76131 Karlsruhe, Germany

T. Kubar

Institute for Physical and Theoretical Chemistry,
Technical University Braunschweig,38106, Braunschweig, Germany

(Dated: October, 01 2009)

Abstract

Charge transport through a short DNA oligomer (Dickerson dodecamer) in presence of structural fluctuations is investigated using a hybrid computational methodology based on a combination of quantum mechanical electronic structure calculations and classical molecular dynamics simulations with a model Hamiltonian approach. Based on a fragment orbital description, the DNA electronic structure can be coarse-grained in a very efficient way. The influence of dynamical fluctuations arising either from the solvent fluctuations or from base-pair vibrational modes can be taken into account in a straightforward way through time series of the effective DNA electronic parameters, evaluated at snapshots along the MD trajectory. We show that charge transport can be promoted through the coupling to solvent fluctuations, which gate the onsite energies along the DNA wire.

PACS numbers: 05.60.Gg 87.15.-v, 73.63.-b, 71.38.-k, 72.20.Ee, 72.80.Le, 87.14.Gg

I. INTRODUCTION

The electrical response of DNA oligomers to applied voltages is a highly topical issue which has attracted the attention of scientists belongig to different research communities. The variability of experimental results is reflected in DNA being predicted to be an insulator,[1] a semiconductor,[2,3] or a metallic-like system.[4,5] This fact hints not only at the difficulties encountered in carrying out well-controlled single-molecule experiments, but also at the dramatic sensitivity of charge migration through DNA molecules to intrinsic, system-related or extrinsic, set-up mediated factors: the specific base-pair sequence, internal vibrational excitations, solvent fluctuations, and the electrode-molecule interface topology, among others. As a result, the theoretical modelling of DNA quantum transport remains a very challenging issue that has been approached from many different sides, see *e.g.*, Refs. [6,7,8,9] for recent reviews. While most of the models originally used started from a static picture of the DNA structure,[10,11,12,13] it has become meanwhile clearer that charge migration through DNA oligomers attached to electrodes may only be understood in the context of a *dynamical approach*.[14,15,16,17,18,19,20,21] Hole transfer experiments[22,23,24,25,26] had already hinted at the strong influence of DNA structural fluctuations in supporting or hindering charge propagation. Hence, it seems natural to expect that dynamical effects would also play a determining role in charge transport processes for molecules contacted by electrodes. A realistic inclusion of the influence of dynamical effects onto the transport properties can however only be achieved via hybrid methodologies combining a reliable description of the biomolecular dynamics and electronic structure with quantum transport calculations. *Ab initio* calculations for static biomoecular structures can provide a very valuable starting point for the parametrization of model Hamiltonians;[27,28,29,30,31,32,33,34,35] however, a full first-principle treatment of both dynamics and electronic structure lies outside the capabilities of state-of-the-art methodologies.

In this paper, we will ellaborate on a recent study on homogeneous DNA sequences[20] by addressing in detail some methodological issues. Our focus will be on the so called Dickerson dodecamer[36] with the sequence $3'-\text{GCGCTTAACGGC}-5'$ and for which the effect of the dynamical fluctuations becomes very clear. Our approach combines classical molecular dynamics (MD) simulations with electronic structure calculations to provide a realistic starting point for the description of the influence of structural fluctuations onto the electronic

structure of a biomolecule. Further, the information drawn from such calculations be used to formulate low-dimensional effective Hamiltonians to describe charge transport. A central point is the use of the concept of fragment orbitals[37,38,39,40] which allows for a very efficient and flexible mapping of the electronic structure of a complex system onto a much simpler effective model. Taking a single base pair as a fragment and considering only one fragment orbital per base pair, we end up in a tight-binding Hamiltonian for a linear chain where both onsite energies $\epsilon_j(t)$ and electronic coupling terms $V_{j,j+1}(t)$ are time-dependent variables:

$$H = \sum_j \epsilon_j(t) d_j^\dagger d_j + \sum_j V_{j,j+1}(t) (d_j^\dagger d_{j+1} + \mathrm{h.}c.). \qquad (1)$$

The dynamical information provided in this way builds the starting point of our treatment of quantum transport through biomolecular wires. In the next Section, we briefly describe the computational methodology used to obtain the effective electronic parameters of the model Hamiltonian, which will be then introduced in Sec. **III**, where we also illustrate how to relate the Hamiltonian of Eq. (1) to a different model describing the coupling of a time-independent electronic system to a bosonic bath. Further, expressions for the electrical current as well as the relation between the auto-correlation function of the onsite energy fluctuations and the spectral density of the bosonic bath will be derived. Finally, we discuss in Sec. **IV** the transport properties of the Dickerson dodecamer in vacuum and in presence of a solvent. We stress that in contrast to other models which explicitly contain the coupling to vibrational excitations or to an environment[41,42,43,44,45] at the price of introducing several free parameters, our methodology potentially contains the full dynamical complexity of the biomolecule as obtained from the MD simulations. One main advantage of our approach is the possibilty to progressively improve the degree of coarse-graining by an appropriate re-definition of the molecular fragments.

II.   MOLECULAR DYNAMICS AND MODEL HAMILTONIAN FORMULATION

A.   Computational methodology

We will first give an overview of the fragment-orbital approach used in our computations; further details can be found elsewhere.[38,39,46]

The core of our method is based on a combination of a charge self-consistent density-functional parametrized tight-binding approach (SCC-DFTB) and the fragment orbital
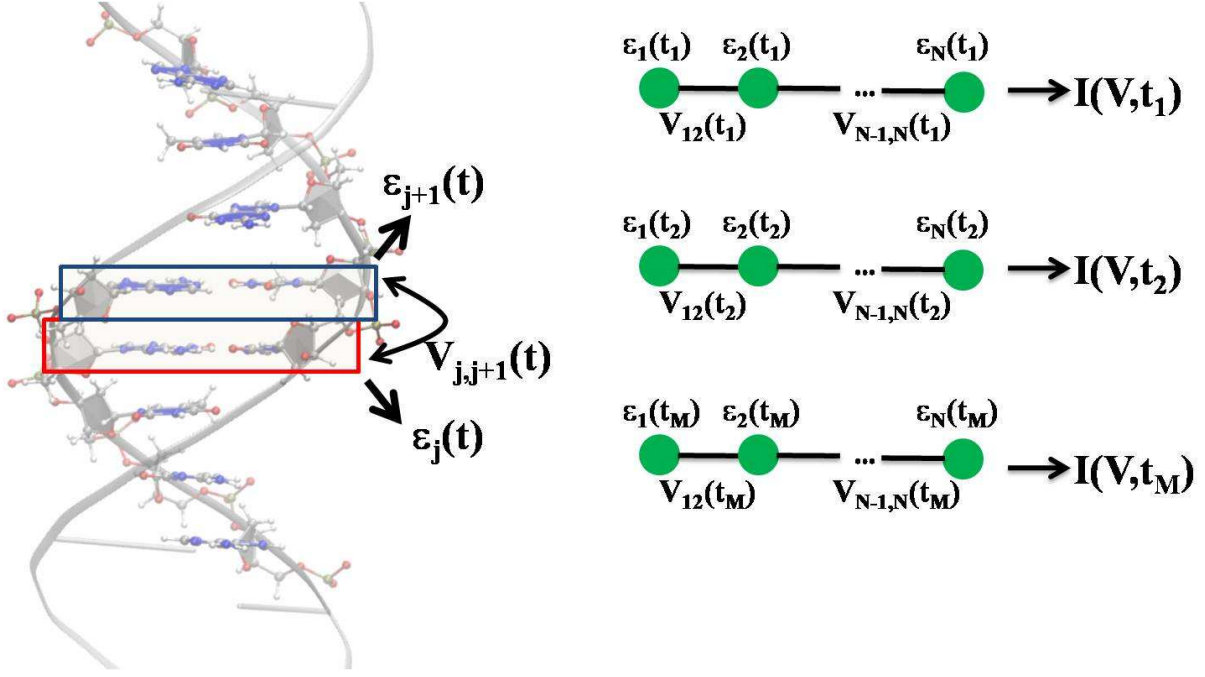
FIG. 1: Left panel: Schematic representation of the fragment orbital method used to perform a coarse-graining of the DNA electronic structure. A fragment consists of a single base pair (not including the sugar phosphate backbones). As explained in the text, the hopping matrix elements $V_{j,j+1}$ between nearest-neighbor fragments are compued using the molecular orbital basis of the isolated base pairs. These calculations are then carried out at snapshots along the molecular dynamics trajectory hence leading to time dependent electronic structure parameters. By keeping only one relevant orbital per fragment, the electronic structure can be mapped onto that of a linear chain (right panel). Transport observables can be computed at each simulation time step. Alternatively, the time dependence o the electronic structure (related to structural and solvent fluctuations) can be transferred to a bosonic bath as done in this paper.

concept;[46] both are used to compute the electronic parameters $\epsilon_j(t)$ and $V_{j,j+1}(t)$ for the effective tight binding model introduced in Eq. (1) in a very efficient way, see Fig. 1 for a schematic representation. The $V_{j,j+1}$ are calculated using the highest occupied molecular orbital Φ_i computed for isolated bases as $V_{j,j+1} = \langle \Phi_j | H | \Phi_{j+1} \rangle$, where the Φ_j's can be expanded in a valence atomic orbital basis η_μ on a given fragment: $\Phi_j = \sum_\mu c_\mu^j \eta_\mu$. The c_μ^j are obtained from calculations on isolated bases and stored for subsequent use to calculate

$V_{j,j+1}$. Therefore, one can write:

$$V_{j,j+1} = \sum_{\mu} \sum_{\nu} c_{\mu}^{j} c_{\nu}^{j+1} \langle \eta_{\mu} | H | \eta_{\nu} \rangle . \tag{2}$$

The Hamilton matrix in the atomic orbital basis $H_{\mu\nu} = \langle \eta_{\mu} | H | \eta_{\nu} \rangle$ evaluated using the SCC-DFTB Hamiltonian matrix is pre-calculated and stored, thus making this step extremely efficient, $i.e.$, it can be calculated for geometry snapshots generated by a classical molecular dynamics simulation even for several nanoseconds. Additionally, the minimal LCAO basis set used in the standard SCC-DFTB code has been optimized for the calculation of the hopping matrix elements,[38,39] and the results are in very good agreement with other approaches.[28,46] Concerning now the coupling to the solvent, a hybrid quantum mechanics/molecular mechanics (QM/MM) approach has been used, implemented in the SCC-DFTB code,[47] leading to the following Hamiltonian matrix in the valence atomic orbital basis η_{ν}:

$$H_{\mu\nu}^{\text{QM/MM}} = H_{\mu\nu}^{\text{SCC-DFTB}} + \frac{1}{2} S_{\mu\nu} \left\{ \sum_{\delta} Q_{\delta} \left(\frac{1}{R_{\alpha\delta}} + \frac{1}{R_{\beta\delta}} \right) + \sum_{A} Q_{A} \left(\frac{1}{r_{A\alpha}} + \frac{1}{r_{A\beta}} \right) \right\} . \tag{3}$$

Here, Q_{δ} are the Mulliken charges of the quantum-mechanical region and the Q_A are the charges in the MM region (backbones, counter-ions, and water), $S_{\mu\nu}$ is the atomic orbital overlap matrix, $H_{\mu\nu}^{\text{SCC-DFTB}}$ is the corresponding zero-order Hamiltonian matrix, and $R_{\alpha\delta}$ is the distance between the DNA atom where the AO orbital η_{μ} is located and the MM atom in the solvent with charge Q_{δ}. The last term explicitly takes into account the coupling to the environment (solvent). The $\epsilon_j = V_{jj}$ and $V_{j,j\pm1}$ from Eq. (2) using Eq. (3) can now be calculated along the MD trajectories[21,39]. The off diagonal matrix elements strongly depend on structural fluctuations of the DNA base pairs, but they are only weakly affected by the solvent dynamics, the opposite holding for the onsite energies which are considerably modified by solvent fluctuations.[21,39] The Fourier transform of the onsite energies autocorrelation function provides information about the spectral ranges which are more strongly contributing to the fluctuations of the electronic parameters, see also the next sections. Thus, we have found that the apparently most important modes are located around 1600 cm^{1} corresponding to a base skeleton mode, and at 800 cm^{-1} related to the water modes.[39] Both contributions modulate the onsite energies significantly on a short time scale and a long time scale of about 1 ps, respectively.

B. Model Hamiltonian for electronic transport

Using Eq. (1) directly for quantum transport calculations may mask to some degree different contributions (solvent, base dynamics) to charge propagation through the DNA π-stack. Moreover, since Eq. (1) contains random variables through the time series, we are confronted with the problem of dealing with charge transport in an stochastic Hamiltonian. This is a more complex task which has been addressed $e.g.$, in the context of exciton transport[48,49,50,51] but also to some degree in electron transfer theories.[52,53,54] Here, we adopt a different point of view and formulate a model Hamiltonian, where the relevant electronic system, in this case the fragment orbital-derived effective DNA electronic system, is coupled explicitly to a bosonic bath. The latter will encode through its spectral density the dynamical information drawn from the MD simulations on internal base dynamics as well as solvent fluctuations. The Hamiltonian can be written in the following way:

$$H = \sum_j \langle \epsilon_j \rangle_t d_j^\dagger d_j - \sum_j \langle V_{j,j+1} \rangle_t \left(d_j^\dagger d_{j+1} + \text{h.c.} \right) \tag{4}$$
$$+ H_{\text{bath}} + H_{\text{el-bath}} + H_{\text{tunnel}} + H_{\text{leads}}$$

$$H_{\text{bath}} = \sum_\alpha \Omega_\alpha B_\alpha^\dagger B_\alpha$$

$$H_{\text{el-bath}} = \sum_{\alpha,j} \lambda_\alpha d_j^\dagger d_j (B_\alpha + B_\alpha^\dagger)$$

$$H_{\text{tunnel}} = \sum_{\mathbf{k},s,j} \left(t_{\mathbf{k}s,j} c_{\mathbf{k}s}^\dagger d_j + \text{h.c.} \right)$$

$$H_{\text{leads}} = \sum_{\mathbf{k},s} \epsilon_{\mathbf{k}s} c_{\mathbf{k}s}^\dagger c_{\mathbf{k}s}$$

The time averages (over the corresponding time series) of the electronic parameters $\langle \epsilon_j \rangle_t$ and $\langle V_{j,j+1} \rangle_t$ have been split off to provide a zero-order Hamiltonian which contains dynamical effects in a mean-field-like level. The effect of the fluctuations around these averages is hidden in the vibrational bath, which is assumed to be a collection of a large $(N \to \infty)$ number of harmonic oscillators in thermal equilibrium at temperature $k_B T$. The bath will be characterized by a spectral density $J(\omega)$ which can also be extracted from the MD simulations, as shown below and in Ref.[55]. Since we are interested in calculating the electrical response of the system, the charge-bath model has to also include the coupling of the system to electronic reservoirs (electrodes). The coupling to the electrodes will be treated in a standard way, using a tunneling Hamiltonian H_{tunnel} which describes the coupling to the s-

lead with $s=$ left (L) or right (R). Later on, the so called wide-band limit will be introduced (the corresponding electrode self-energies are purely imaginary and energy-independent), thus reducing the electrode-DNA coupling to a single parameter.

The previous model relies on some basic assumptions that can be substantiated by the results of the MD simulations:[39] (i) The complex DNA dynamics can be well mimic within the harmonic approximation by using a continuous vibrational spectrum; (ii) The simulations show that the local onsite energy fluctuations are much stronger in presence of a solvent than those of the electronic hopping integrals (see also the end of the previous section), so that we assume that the bath is coupled only diagonally to the charge density fluctuations; (iii) Fluctuations on different sites display rather similar statistical properties, so that the charge-bath coupling λ_α is taken to be independent of the site j. This latter approximation can be lifted by introducing additional site-nonlocal spectral densities $J_{j,j+1}(\omega)$; this however would make the theory more involved and less transparent. In Fig. 2 we show typical normalized auto-correlation functions of the onsite energy fluctuations for the Dickerson dodecamer in both solvent and vacuum conditions as well as one case of off-diagonal correlations between nearest-neighbor site energies (inset). Also shown are fits to stretched exponentials, which are in general equivalent to a sum of simple exponential functions. This suggests the presence of different time scales and the non-trivial time-dependence of the fluctuation dynamics. The fits become obviously less accurate at long times due to the reduced number of sampled data points with increasing time (the oscillatory behavior becomes stronger). From the figure we first see that the off-diagonal correlations decay on a much shorter time scale as the local ones, so that on a first approximation their neglection can be justified; further the decay of the correlations for the vacuum simulations is considerably much faster than in a solvent indicating the strong influence of the latter in gating the electronic structure of the biomolecule. The corresponding correlation functions for the hopping integrals $V_{j,j+1}(t)$ (not shown) display even shorter relaxation times, so that the approximation $V_{j,j+1}(t) = \langle V_{j,j+1}(t) \rangle_t$ is enough for our purposes (the hopping integrals are self-averaging).

In order to deal with the previous model, we first perform a polaron transformation of the Hamiltonian Eq. (4), using the generator $\mathcal{U} = \exp[\sum_{\ell,\alpha} g_\alpha d_\ell^\dagger d_\ell (B_\alpha^\dagger - B_\alpha)]$, which is nothing else as a shift operator of the harmonic oscillators equilibrium positions. The parameter $g_\alpha = \lambda_\alpha/\Omega_\alpha$ gives an effective measure of the electron-vibron coupling strength. Since we will work in the wide-band limit for the electrode self-energies, the renormalization of the
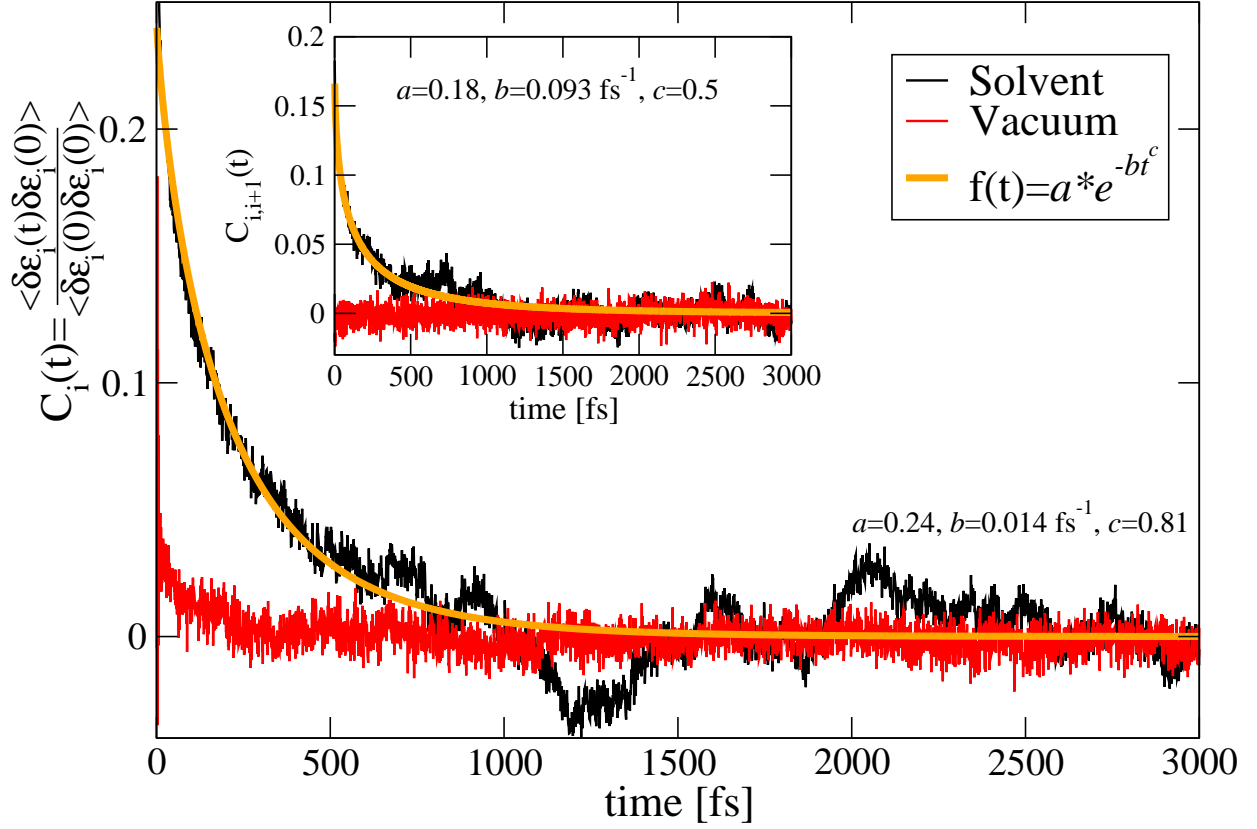
FIG. 2: Normalized auto-correlation function[55] $C_i(t) = \langle \delta\epsilon_i(t)\delta\epsilon_i(0) \rangle / \langle \delta\epsilon_i^2 \rangle$ and averaged nearest-neighbor correlation function $C_{i,i+1}(t) = \langle \delta\epsilon_i(t)\delta\epsilon_{i+1}(0) \rangle / \langle \delta\epsilon_i\delta\epsilon_{i+1} \rangle$ (inset) of the onsite energy fluctuations. The solid lines are fits to stretched exponentials which suggests the existence of different time scales, a typical situation in the dynamics of bio-molecules. On average, the decay of $C_{i,i+1}(t)$ occurs on a much shorter time scale than that of $C_i(t)$, so that our model will only include in a first approximation local fluctuations, see Eq. (1).

tunneling Hamiltonian by a vibronic operator will be neglected. As a result, we obtain a Hamiltonian with decoupled electronic and vibronic parts and where the onsite energies are shifted as $\langle \epsilon_j \rangle_t \to \langle \epsilon_j \rangle_t - \int_0^\infty d\omega J(\omega)/\omega$. However, as it is well-known,[56] the retarded Green function of the system is now an entangled electronic-vibronic object that can not be treated

exactly; we thus decouple it in the approximate way:[41,57]

$$\begin{aligned}
\mathcal{G}_{nm}(t,t') &= -i\,\theta(t-t')\left\langle \left[d_n(t)\mathcal{X}^\dagger(t), d_m^\dagger(t')\mathcal{X}(t')\right]_+\right\rangle \quad (5)\\
&\approx -i\,\theta(t-t')\left\{\left\langle d_n(t)d_m^\dagger(t')\right\rangle\left\langle \mathcal{X}^\dagger(t)\mathcal{X}(t')\right\rangle + \left\langle d_m^\dagger(t')d_n(t)\right\rangle\left\langle \mathcal{X}(t')\mathcal{X}^\dagger(t)\right\rangle\right\}\\
&= \theta(t-t')\left\{G_{nm}^>(t,t')e^{-\phi(t-t')} - G_{nm}^<(t,t')e^{-\phi(t'-t)}\right\}\\
\phi(t) &= \sum_\alpha (\frac{\lambda_\alpha}{\Omega_\alpha})^2\left[(1+N_\alpha)e^{-i\Omega_\alpha t} + N_\alpha e^{+i\Omega_\alpha t}\right]
\end{aligned}$$

In this equation, $\theta(t-t')$ is the Heaviside function and the pure bosonic operator $\mathcal{X}(t) = \exp[\sum_\alpha g_\alpha(B_\alpha^\dagger - B_\alpha)]$. In the last row of Eq. (5) we can pass to the continuum limit and express $\phi(t)$ in terms of the bath spectral density $J(\omega)$:[58]

$$\phi(t) = \frac{1}{\hbar}\int_0^\infty d\omega\,\frac{J(\omega)}{\omega^2}\coth\frac{\hbar\omega}{k_B T}(1-\cos\omega\,t) - i\frac{1}{\hbar}\int_0^\infty d\omega\frac{J(\omega)}{\omega^2}\sin\omega\,t. \quad (6)$$

C. The electrical current

We derive in this section the expression we are going to use to calculate the electrical current through the DNA oligomer under study. Starting point is the well-known Meir-Wingreen expression for the current from lead s:[59]

$$I_s = \frac{2e}{\hbar}\int\frac{dE}{2\pi}\,\mathrm{Tr}\left\{\Sigma_s^<(E)G^>(E) - \Sigma_s^>(E)G^<(E)\right\}.$$

Now, we can exploit the decoupling approximation used in Eq. (5) together with the wide-band limit in the electrode-molecule coupling to write e.g., for the left electrode:

$$\begin{aligned}
\Sigma_L^<(E)G^>(E) &= \int\frac{dE'}{2\pi}\,f_L(E)(1-f_R(E'))t(E')\Phi(E-E'),\\
\Sigma_L^>(E)G^<(E) &= \int\frac{dE'}{2\pi}\,(1-f_L(E))f_R(E')t(E')\Phi(E'-E),\\
\Phi(E) &= \int\frac{dt}{\hbar}\,e^{\frac{i}{\hbar}Et}e^{-\phi(t)}.
\end{aligned}$$

Hereby we have used the explicit expressions for the greater- and lesser-Green functions:

$$\mathbf{G}_0^{>,<}(E) = \mathbf{G}_0(E)(\mathbf{\Sigma}_L^{>,<}(E) + \mathbf{\Sigma}_R^{>,<}(E))\mathbf{G}_0^\dagger(E), \quad (7)$$

the index 0 indicating that the vibrational degrees of freedom have already been decoupled. The transmission-like function $t(E)$ is given by $t(E) = \mathrm{Tr}\left\{\mathbf{G}_0(E)\mathbf{\Gamma}_L\mathbf{G}_0^\dagger(E)\mathbf{\Gamma}_R\right\}$. The

retarded matrix Green function $\mathbf{G}_0(E)$ is calculated without electron-bath coupling but including the interaction with the electrodes: $\mathbf{G}_0^{-1}(E) = E + \mathrm{i}\,\eta - \mathbf{H}_0 + \mathrm{i}\,\mathbf{\Gamma}_\mathrm{L} + \mathrm{i}\,\mathbf{\Gamma}_\mathrm{R}$, $\mathbf{H}_0$ being the electronic part of the Hamiltonian of Eq. (4). Using these results, the right-going current can be written as

$$I_\mathrm{L} = \frac{2e}{\hbar} \int \frac{dE}{2\pi} \int \frac{dE'}{2\pi}\, t(E')\, \{f_\mathrm{L}(E)(1 - f_\mathrm{R}(E'))\Phi(E - E') - (1 - f_\mathrm{L}(E))f_\mathrm{R}(E')\Phi(E' - E)\} \ (8)$$

a similar expression holding for the left-going current, when the indices L and R are interchanged. The total current can be written in a symmetrized way: $I_\mathrm{T} = (I_\mathrm{L} - I_\mathrm{R})/2$. By looking at Eq. (6), two limiting cases can immediately be obtained: the zero charge-bath coupling ($\phi = 0$) which implies $\Phi(E) = 2\pi\delta(E)$. In this limit we recover the conventional expression for coherent transport, involving only the transmission function $t(E)$. In the high-temperature and/or strong coupling limit to the bath, a short-time expansion of $\phi(t)$ can be performed, yielding:

$$\begin{aligned}
\phi(t) &= \frac{t^2}{2\hbar} \int_0^\infty d\omega\, J(\omega) \coth \frac{\hbar\omega}{k_\mathrm{B}T} - \mathrm{i}\frac{t}{\hbar} \int_0^\infty d\omega \frac{J(\omega)}{\omega}, \\
&= \kappa_\mathrm{therm} t^2 - \mathrm{i}\frac{E_\mathrm{reorg}}{\hbar} t.
\end{aligned}$$

In the former expression $\sqrt{\kappa_\mathrm{therm}}$ is related to an inverse decoherence time. In the high temperature limit $\kappa_\mathrm{therm} \sim k_\mathrm{B}T E_\mathrm{reorg}$. The Fourier transform of the previous expression can be calculated straightforward and gives:

$$\Phi(E) = \sqrt{\frac{\pi}{\hbar^2 \kappa_\mathrm{therm}}} \exp\left[-\frac{(E + E_\mathrm{reorg})^2}{4\hbar^2 \kappa_\mathrm{therm}}\right].$$

Thus, the current calculated using Eq. (8) becomes a convolution of $t(E)$ with a Gaussian function. Notice the similarity of this expression with a Frank-Condon factor appearing in the Marcus electron transfer theory.

D. Spectral density from molecular dynamics

The next issue at stake is how to relate the bath spectral density $J(\omega)$ to the time series of the electronic parameters as obtained through the molecular dynamic simulations. To illustrate this point we will consider the simple case of a single level, whose site energy is a Gaussian random variable, coupled to left and right electrodes according to the Hamiltonian

(we assume for simplicity that $\langle \epsilon(t) \rangle = 0$):

$$H = \delta\epsilon(t)d^\dagger d + H_{\text{tunnel}} + H_{\text{leads}} \tag{9}$$

To deal with this problem we may use equation of motion techniques for the retarded dot Green function $G(t,t') = -(\mathrm{i}/\hbar)\theta(t-t')\left\langle\{d(t),d^\dagger(t')\}\right\rangle$ in the time domain:

$$(\mathrm{i}\,\hbar\partial_t - \delta\epsilon(t))G(t,t') = \delta(t-t') + \sum_{\mathbf{k},\alpha} t^\dagger_{\mathbf{k},\alpha}G_{\mathbf{k}\alpha}(t,t'), \tag{10}$$

with $G_{\mathbf{k}\alpha}(t,t') = -(\mathrm{i}/\hbar)\theta(t-t')\left\langle\{c_{\mathbf{k},\alpha}(t),d^\dagger(t')\}\right\rangle$. A similar equation of motion for the latter function allows to introduce the electrode self-energies:

$$(\mathrm{i}\,\hbar\partial_t - \delta\epsilon(t))G(t,t') = \delta(t-t') + \int d\tau\Sigma(t,\tau)G(\tau,t'),$$
$$\Sigma(t,\tau) = \sum_{\mathbf{k},\alpha}|t_{\mathbf{k},\alpha}|^2 e^{-\mathrm{i}\,\epsilon_{\mathbf{k},\alpha}t} \tag{11}$$

Note that the Green function thus obtained is still a random function, since no average over the random variable $\delta\epsilon(t)$ has been yet performed. Using the wide-band limit in the lead self-energies $\Sigma_\alpha(t,t') = -\mathrm{i}\,\Gamma_\alpha\delta(t-t')$ we get, with $\Gamma = \Gamma_L + \Gamma_R$:

$$(\mathrm{i}\,\hbar\partial_t - \delta\epsilon(t) + \mathrm{i}\,\Gamma)G(t,t') = \delta(t-t'). \tag{12}$$

Introducing the time-exponential $\mathcal{U}(t,t') = \exp(-(\mathrm{i}/\hbar)\int_{t'}^t ds(\delta\epsilon(t) - \mathrm{i}\,\Gamma)$ allows to write a closed solution for the dot's Green function:

$$G(t,t') = -\frac{\mathrm{i}}{\hbar}\theta(t-t')\mathcal{U}(t,t') \tag{13}$$

The average Green function over the random variable $\delta\epsilon(t)$ yields now in energy-space:

$$\langle G(E)\rangle = -\frac{\mathrm{i}}{\hbar}\int_0^\infty dt\, e^{\frac{\mathrm{i}}{\hbar}E(t-t')}\langle\mathcal{U}(t-t')\rangle = -\mathrm{i}\int_0^\infty dt e^{\frac{\mathrm{i}}{\hbar}(E+\mathrm{i}\Gamma)(t-t')}\left\langle e^{-\frac{\mathrm{i}}{\hbar}\int_{t'}^t ds\delta\epsilon(s)}\right\rangle. \tag{14}$$

Performing now a cumulant expansion[60] of the averaged exponential and taking into account that cumulants higher than the second one exactly vanish due to the Gaussian nature of the fluctuations and to the fact that $\delta\epsilon(t)$ is a classical variable, we get (with $t' = 0$):

$$\langle G(E)\rangle = -\frac{\mathrm{i}}{\hbar}\int_0^\infty dt\, e^{\frac{\mathrm{i}}{\hbar}(E+\mathrm{i}\Gamma)t}\, e^{-\frac{1}{\hbar^2}\int_0^t ds\int_0^s ds'\,\langle\delta\epsilon(s)\delta\epsilon(s')\rangle}, \tag{15}$$

which is the formally exact solution of the problem. We may now look at the same problem from a different point of view by considering *explicitly* the coupling of a single site with

11

time-independent onsite energy to a continuum of vibrational excitations. Using the polaron transformation together with the approximations introduced at the beginning of Sec. **II B**, we can write the retarded Green function as:

$$G(E) = -\frac{i}{\hbar} \int_0^\infty dt \, e^{\frac{i}{\hbar}(E+i\Gamma)t} \, e^{-\phi(t)},$$ (16)

where $\phi(t)$ has been already defined in Eq. (6). By comparison of Eqs.(15) and (16), there must exist a relation between the (real) correlation function and the real part of $\phi(t)$. The latter can be re-written in the following way:

$$\begin{aligned} \mathrm{Re}\,\phi(t) &= \frac{1}{\hbar} \int_0^\infty d\omega \, \frac{J(\omega)}{\omega^2} \coth\frac{\hbar\omega}{k_B T}(1 - \cos\omega\,t) \\ &= \int_0^t ds \int_0^s ds' \left\{ \frac{1}{\hbar} \int_0^\infty d\omega\, J(\omega) \coth\frac{\hbar\omega}{k_B T} \cos\left[\omega\left(s - s'\right)\right] \right\}, \end{aligned}$$

so that from this we conclude that

$$\langle \delta\epsilon(s)\delta\epsilon(s') \rangle = \hbar \int_0^\infty d\omega\, J(\omega) \coth\frac{\hbar\omega}{k_B T} \cos\left[\omega\left(s - s'\right)\right].$$

From here it follows by inversion:

$$J(\omega) = \frac{2}{\pi\hbar} \tanh\frac{\hbar\omega}{k_B T} \int_0^\infty dt\, \cos\omega t\, C(t) = \frac{2}{\pi\hbar} \tanh\frac{\hbar\omega}{k_B T} j(\omega).$$ (17)

The previous result was obtained in Ref. 55 in the weak coupling, perturbative regime to the vibrational system; we have shown here that it can be also extended to the case of arbitrary coupling. Similar expressions could be derived for (spatially) non-local spectral densities.

E.   Results

To illustrate our methodology we have focused on the Dickerson dodecamer (DD) which has a non-homogeneous base sequence. In contrast to our previous study[20] where homogeneous DNA sequences were addressed like poly(G)-poly(C) and poly(A)-poly(T), the study of the DD nicely illustrates the role of the solvent fluctuations in gating the electronic structure. To study the effect of the conformational dynamics as well as the fluctuations of environment onto the charge transport properties, we have performed classical MD simulations using the AMBER-parm99 force field92 with the parmBSC0 extension93 as implemented in the GROMACS[61] software package. The static geometries were built with the 3DNA program[62]
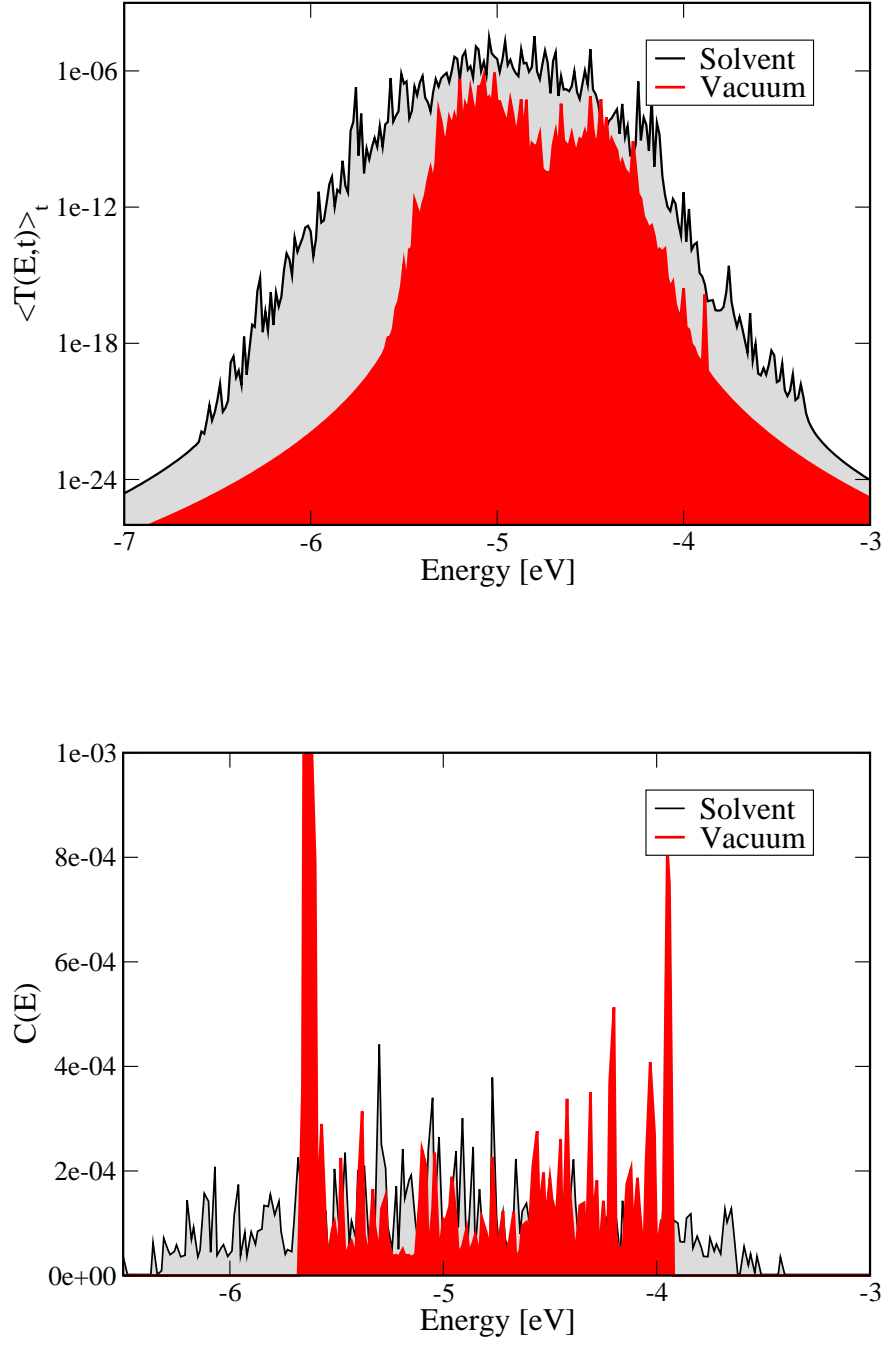
FIG. 3: Upper panel: Time averaged transmission function for simulations performed in solvent and in vacuum. Lower panel: Coherence parameter $C(E)$ for the Dickerson dodecamer in solvent and in vacuum. Notice that the influence of the solvent fluctuations is to spread out the spectral support of $C(E)$. As expected, the coherence parameter is on average larger for the vacuum case where a large part of the fluctuations is suppressed due to the absence of an environment. Nevertheless the transmission in the vacuum case is much smaller, nicely illustrating the positive influence of the environment in gating charge migration.
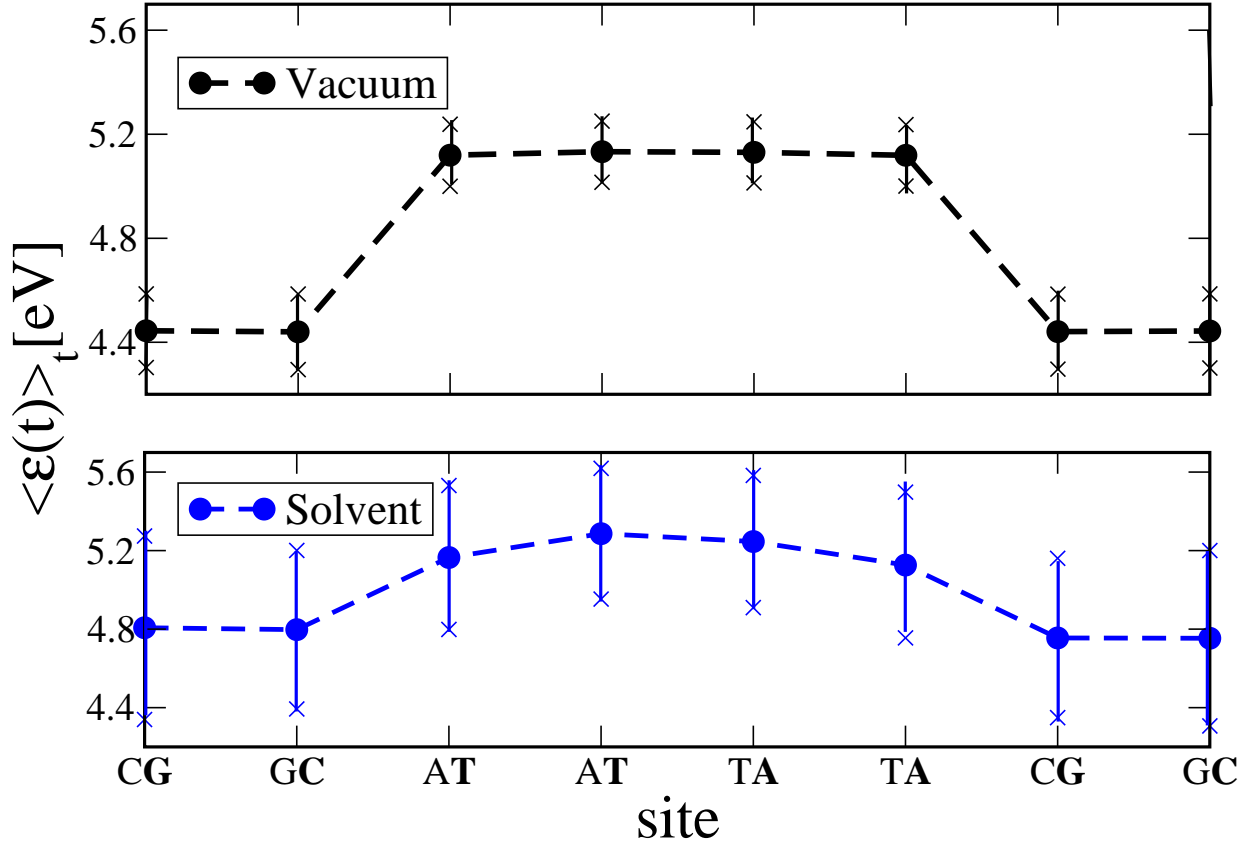
FIG. 4: Time averaged of the absolute value of the onsite energies along the segment covering bases 3 and 10 of the Dickerson dodecamer, *i.e.*, over the sequence $3'-$GC**GCTTAACG**GC$-5'$) for simulations in vacuum (upper panel) and in solvent (lower panel). The outer most two bases on each end were not included in the calculations to avoid undesired boundary effects. The averaged energy profile in presence of the solvent becomes smoother but also the fluctuations around the averages are stronger. This smoothing reduces the energy barriers between the sites and hence favours charge migration.

while the starting structures for the MD simulations were created using the make-na server.[63] After a standard heating procedure followed by a 1 ns equilibration phase, we performed 30 ns MD simulations with a time step of 2 fs. The simulations were carried out in a rectangular box with periodic boundary conditions and filled with 5500 TIP3P water molecules and 22 sodium counterions for neutralization. Snapshots of the molecular structures were saved every 1 ps, for which the charge transfer parameters were calculated with the methodology described in the previous sections. When speaking of simulations in vacuum conditions, we mean that the last term in Eq. 3 is left out. Upon mapping the electronic structure
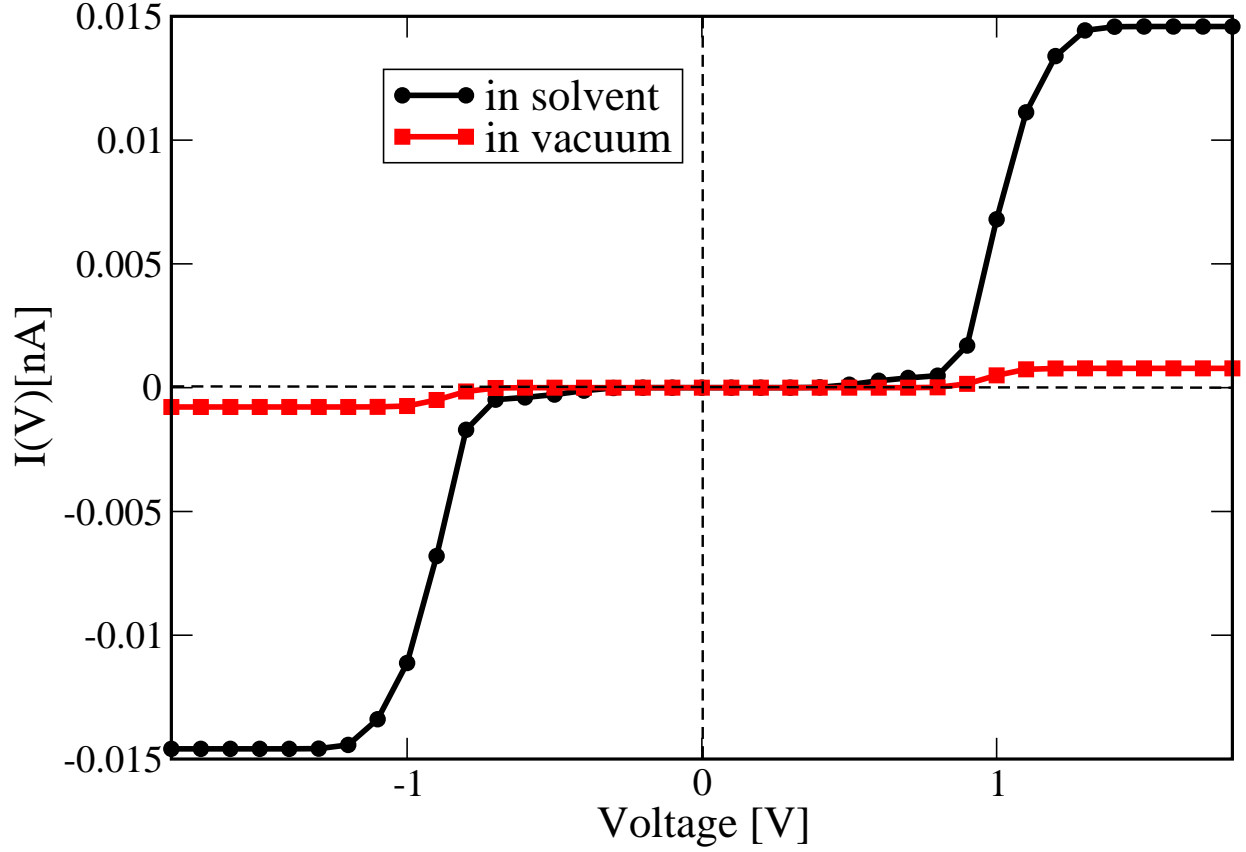
FIG. 5: Electrical current for seven base pairs of poly(dG)-poly(dC) and poly(dA)-poly(dT) oligomers in vacuum. The current is considerably suppressed when comparing with the case where solvent fluctuations are included.

onto a linear chain as discussed in the former sections, we have first computed the time and energy dependent quantum-mechanical transmission function $T(E,t)$ by evaluating for every set of charge transfer parameters, i.e., at each simulation time step t, $\langle T(E,t) \rangle_t = (1/T_{\mathrm{MD}}) \sum_j T(E,t_j)$. This quantity is expected to provide some qualitative insight into different factors affecting transport (solvent vs. vacuum) but its use is restricted by the fact that for longer chains inelastic, fluctuation mediated channels will play an increasing role and then a pure elastic transmission can not catch all the transport physics. In this latter case, the model Eq. (5) seems to us more appropriate since it includes the dressing of the electronic degrees of freedom by the structural fluctuations. In Fig. 3 we show the averaged transmission function (upper panel) for the cases where solvent effects are included or neglected, respectively. We clearly see that solvent-mediated fluctuations considerably increase and broaden the transmission spectrum. Its fragmented structure is simply due to

15

the fluctuations in the onsite energies, which make the system effectively highly disordered. Another way of looking at the effect of fluctuations is via the introduction of a coherence parameter[20] which is defined as $C(E) = \langle T(E,t) \rangle_t^2 / \langle T(E,t)^2 \rangle_t$. If the fluctuations are weak $C(E$ goes to one, while a strong fluctuating system will lead to a considerably reduction of $C(E)$. Obviously, this parameter has only a clear meaning over the spectral support of the transmission function. $C(E)$ is shown in the lower panel of Fig. 3; the coherence parameter in vacuum conditions can become larger than in solvent for some small energy regions due to the reduction of the fluctuations. However, this does not turn to be enough to increase the transport efficiency for the special base sequence of the Dickerson DNA, since this system has in the static limit a distribution of energetic barriers due to the base pair sequence. To further illustrate the influence of the solvent, we have plotted in Fig. 4 the time averaged onsite energies along the model tight-binding chain. Remarkably, the presence of the solvent "smoothes" the averaged energy profile (though the amplitude of the fluctuations clearly becomes stronger). To compute the current through the system, we use the Hamiltonian Eq. (5) and the current expression, Eq. (8), derived with this model. The Fermi energy in these calculations was fixed at the upper edge of the transmission spectrum, see Fig. 3. The qualitative results are however not considerably changed by slightly changing its position. In Fig. 5 the current is shown for the two cases of interest. Due to the presence of tunnel barriers in the wire which are not fully compensated on average by the gating effect of the environment, the absolute current values are rather small when compared with those of homogeneous sequences[20]. However, the current including the solvent is roughly fifteen times larger than for that obtained from the simulations in vacuum. Though our model Hamiltonian in Eq. (5) does not fully contain all the dynamical correlations encoded in the time dependent electronic parameters, we nevertheless expect that their inclusion would lead to an even further increase of the difference between solvent and vacuum results, thus suppporting our main conclusions.

III. CONCLUSIONS

We have presented a hybrid methodology which allows for a very efficient coarse-graining of the electronic structure of complex biomolecular systems as well as to include the influence of structural fluctuations into the electronic parameters. The time series obtained in this way

allow to map the problem onto an effective low dimensional model Hamiltonian describing the interaction of charges with a bosonic bath, which comprises the dynamical fluctuations. The possibility to parametrize the bath spectral density $J(\omega)$ using the information obtained from the time series makes our approach very efficient, since we do not need to use the typical phenomenological *Ansätze* (ohmic, Lorentzian, etc) to describe the bath dynamics. The example presented here, the Dickerson dodecamer, shows in a very clear way that solvent-mediated gating may be a very efficient mechanism in supporting charge transport if the static DNA reference structure already posseses a disordered energy profile (due to the base sequence). Our method is obviously not limited to the treatment of DNA but it can equally well be applied to deal with charge migration in other complex systems like molecular organic crystals or polymers, where charge dynamics and coupling to fluctuating environments plays an important role.[52,53,54,64,65,66,67,68]

IV. ACKNOWLEDGMENTS

---

[1] E. Braun, Y. Eichen, U. Sivan, and G. Ben-Yoseph, Nature **391**, 775 (1998).

[2] D. Porath, A. Bezryadin, S. D. Vries, and C. Dekker, Nature **403**, 635 (2000).

[3] H. Cohen, C. Nogues, R. Naaman, and D. Porath, Proc. Natl. Acad. Sci. USA **102**, 11589 (2005).

[4] B. Xu, P. Zhang, X. Li, and N. Tao, Nano Letters **4**, 1105 (2004).

[5] K.-H. Yoo, D. H. Ha, J.-O. Lee, J. W. Park, J. Kim, J. J. Kim, H.-Y. Lee, T. Kawai, and H. Y. Choi, Phys. Rev. Lett. **87**, 198102 (2001).

[6] D. Porath, G. Cuniberti, and R. D. Felice, in *Long-Range Charge Transfer in DNA I and II*, Topics in Current Chemistry **237**, ed. G. B. Schuster (Springer, Berlin, New York, 2004), p.

17

183.

[7] *Modern methods for theoretical physical chemistry of biopolymers*, edited by S. Tanaka, J. Lewis, and E. Starikow (Elsevier, Amsterdam, 2006).

[8] *NanoBioTechnology: BioInspired device and materials of the future*, edited by O. Shoseyov and I. Levy (Humana Press, 2007).

[9] *Charge migration in DNA: perspectives from physics, chemistry and biology*, edited by T. Chakraborty (Springer, Berlin, New York, 2007).

[10] S. Roche, Phys. Rev. Lett. **91**, 108101 (2003).

[11] G. Cuniberti, L. Craco, D. Porath, and C. Dekker, Phys. Rev. B **65**, 241314 (2002).

[12] C.-T. Shih, S. Roche, and R. A. Romer, Phys. Rev. Lett. **100**, 018105 (2008).

[13] A.-M. Guo and S.-J. Xiong, Phys. Rev. B **80**, 035115 (2009).

[14] D. Hennig, E. B. Starikov, J. F. R. Archilla, and F. Palmero, J. Bio. Phys. **30**, 227 (2004).

[15] H. Yamada, E. Starikov, and D. Hennig, Eur. Phys. J. B **59**, 185 (2007).

[16] T. Cramer, S. Krapf, and T. Koslowski, J. Phys. Chem. C **111**, 8105 (2007).

[17] F. C. Grozema, S. Tonzani, Y. A. Berlin, G. C. Schatz, L. D. Siebbeles, and M. A. Ratner, J. Amer. Chem. Soc. **130**, 5157 (2008).

[18] F. Grozema, Y. Berlin, and L. D. A. Siebbeles, J. Amer. Chem. Soc. **122**, 10903 (2000).

[19] A. Troisi and G. Orlandi, J. Phys. Chem. B. **106**, 2093 (2002).

[20] R. Gutierrez, R. Caetano, P. B. Woiczikowski, T. Kubar, M. Elstner, and G. Cuniberti, Phys. Rev. Lett. **102**, 208102 (2009).

[21] P. B. Woiczikowski, T. Kubar, R. Gutierrez, R. Caetano, G. Cuniberti, and M. Elstner, J. Chem. Phys. **130**, 215104 (2009).

[22] E. Meggers, M. E. Michel-Beyerle, and B. Giese, J. Am. Chem. Soc. **120**, 12950 (1998).

[23] E. Meggers, D. Kusch, M. Spichty, U. Wille, and B. Giese, Angew. Chem. Int. Ed. Engl. **37**, 460 (1998).

[24] C. R. Treadway, M. G. Hill, and J. K. Barton, Chem. Phys. **281**, 409 (2002).

[25] N. J. Turro and J. K. Barton, J. Biol. Inorg. Chem. **3**, 201 (1998).

[26] C. Wan, T. Fiebig, S. O. Kelley, C. R. Treadway, and J. K. Barton, Proc. Natl. Acad. Sci **96**, 6014 (1999).

[27] A. Voityuk, N. Rösch, M. Bixon, and J. Jortner, J. Phys. Chem. B **104**, 5661 (2000).

[28] A. A. Voityuk, J. Chem. Phys. **128**, 115101 (2008).

[29] A. A. Voityuk, J. Chem. Phys. **123**, 034903 (2005).

[30] H. Mehrez and M. P. Anantram, Phys. Rev. B **71**, 115405 (2005).

[31] A. Calzolari, R. D. Felice, E. Molinari, and A. Garbesi, Appl. Phys. Lett. **80**, 3331 (2002).

[32] R. D. Felice, A. Calzolari, and E. Molinari, Phys. Rev. B **65**, 045104 (2002).

[33] R. D. Felice, A. Calzolari, and H. Zhang, Nanotechnology **15**, 1256 (2004).

[34] J. P. Lewis, T. E. Cheatham, E. B. Starikov, H. Wang, and O. F. Sankey, J. Phys. Chem. B **107**, 2581 (2003).

[35] J. Ladik, A. Bende, and F. Bogar, J. Chem. Phys. **128**, 105101 (2008).

[36] H. Drew, R. Wing, T. Nakano, C. Broka, S. Tanaka, K. Itakura, and R. E. Dickerson, Proc. Natl. Acad. Sci. USA **78**, 2179 (1981).

[37] K. Senthilkumar, F. C. Grozema, C. F. Guerra, F. M. Bickelhaupt, F. D. Lewis, Y. A. Berlin, M. A. Ratner, and L. D. A. Siebbeles, J. Am. Chem. Soc. **127**, 148094 (2005).

[38] T. Kubar, P. B. Woiczikowski, G. Cuniberti, and M. Elstner, J. Phys. Chem. B **112**, 7937 (2008).

[39] T. Kubar and M. Elstner, J. Phys. Chem. B **112**, 8788 (2008).

[40] B. Song, M. Elstner, and G. Cuniberti, Nano Letters **8**, 3217 (2008).

[41] R. Gutierrez, S. Mohapatra, H. Cohen, D. Porath, and G. Cuniberti, Phys. Rev. B **74**, 235105 (2006).

[42] R. Gutierrez, S. Mandal, and G. Cuniberti, Nano Letters **5**, 1093 (2005).

[43] R. Gutierrez, S. Mandal, and G. Cuniberti, Phys. Rev. B **71**, 235116 (2005).

[44] B. B. Schmidt, M. H. Hettler, and G. Schön, Phys. Rev. B **75**, 115125 (2007).

[45] B. B. Schmidt, M. H. Hettler, and G. Schon, Phys. Rev. B **77**, 165337 (2008).

[46] A. A. Voityuk, K. Siriwong, and N. Rösch, Angew. Chem. Int. Ed. **43**, 624 (2004).

[47] Q. Cui, M. Elstner, E. Kaxiras, T. Frauenheim, and M. Karplus, J. Phys. Chem. B **105**, 569 (2001).

[48] V. M. Kenkre and D. W. Brown, Phys. Rev. B **31**, 2479 (1985).

[49] V. M. Kenkre and D. Schmid, Phys. Rev. B **31**, 2430 (1985).

[50] H. Haken and P. Reineker, Z. Phys. A **249**, 253 (1972).

[51] R. Kühne and P. Reineker, Z. Phys. B **22**, 201 (1975).

[52] S. S. Skourtis, I. A. Balabin, T. Kawatsu, and D. N. Beratan, Proc. Nat. Acad. Sci. **102**, 3552 (2005).

[53] E. Gudowska-Nowak, Chem. Phys. **212**, 115 (1996).

[54] I. A. Goychuk, E. G. Petrov, and V. May, J. Chem. Phys. **103**, 4937 (1995).

[55] A. Damjanovic, I. Kosztin, U. Kleinekathöfer, and K. Schulten, Phys. Rev. E **65**, 031919 (2002).

[56] G. D. Mahan, *Many-Particle Physics*, 3rd ed. (Plenum Press, New York, 2000).

[57] M. Galperin, A. Nitzan, and M. A. Ratner, Phys. Rev. B **73**, 045314 (2006).

[58] U. Weiss, *Quantum Dissipative Systems*, Vol. 10 of *Series in Modern Condensed Matter Physics* (World Scientific, 1999).

[59] Y. Meir and N. S. Wingreen, Phys. Rev. Lett. **68**, 2512 (1992).

[60] R. Kubo, J. Phys. Soc. Jpn. **17**, 1100 (1962).

[61] D. van der Spoel, E. Lindahl, B. Hess, G. Groenhof, A. E. Mark, and H. J. C. Berendsen, J. Comput. Chem. **26**, 1701 (2005).

[62] X. Lu and W. K. Olson, Nucleic Acids Res. **31**, 5108 (2003).

[63] http://structure.usc.edu/make na/server.html.

[64] A. Troisi, D. L. Cheung, and D. Andrienko, Phys. Rev. Lett. **102**, 116602 (2009).

[65] T. F. Soules and C. B. Duke, Phys. Rev. B **3**, 262 (1971).

[66] D. Q. Andrews, R. P. Van Duyne, and M. A. Ratner, Nano Letters **8**, 1120 (2008).

[67] A. Troisi, M. A. Ratner, and M. B. Zimmt, J. Amer. Chem. Soc. **126**, 2215 (2004).

[68] D. J. Bicout and M. J. Field, J. Phys. Chem. **99**, 12661 (1995).